J Radioanal Nucl Chem (2015) 304:527–533
DOI 10.1007/s10967-014-3876-5

# Selective sorption mechanism of $Cs^+$ on potassium nickel hexacyanoferrate(II) compounds

**YunHua Qing · Jun Li · Bin Kang · ShuQuan Chang · YaoDong Dai · Qing Long · Chao Yuan**

Received: 24 June 2014 / Published online: 14 January 2015


**Abstract** Herein, the sorption behavior of potassium nickel hexacyanoferrate(II) (KNiFC) for $Cs^+$ was investigated by sorption kinetics and isotherms. The results indicate sorption isotherms are well described by the Freundlich equation, sorption kinetics agree with pseudo-second-order kinetics, and rate limiting processes are controlled by film diffusion. The distribution coefficient of $Cs^+$ ($K_{d,Cs}$), decreased following the order: $NH_4^+ > K^+ > Na^+ > Ca^{2+} > Mg^{2+}$, and declined with the increase of pH to a minimum value of 5.3 and then increased with the increase of pH. The selective sorption was closely related to hydrated radius, charge-radius, ionization potential and the structure of KNiFC.

Y. Qing · J. Li · B. Kang · S. Chang · Y. Dai (✉) · Q. Long · C. Yuan
Department of Nuclear Science and Technology, College of Material Science and Engineering, Nanjing University of Aeronautics and Astronautics, Nanjing 211106, Jiangsu, People's Republic of China
e-mail: yd_dai@126.com

Y. Qing
e-mail: Yh_qing0907@163.com

J. Li
e-mail: ljiceprince@163.com

B. Kang
e-mail: bin.kang@chemistry.gatech.edu

S. Chang
e-mail: chsq@nuaa.edu.cn

Q. Long
e-mail: 15850535613@163.com

C. Yuan
e-mail: 635620583@qq.com

**Keywords** KNiFC · Ion exchange · $Cs^+$ · Radioactive wastewater

## Introduction

Nuclear energy is a kind of clean energy, and no carbon dioxide is released into air during the nuclear electricity generation. However, significant changes in the global budget of radionuclides in environment have occurred. The subsurface water bodies have been polluted gradually by radionuclides with the development of nuclear plant, nuclear submarine, radioisotope source, nuclear medicine instruments, etc. Recently, Tokyo Electric Power had acknowledged the leak of water storage tank, which was about 300 ton with $8 \times 10^7$ Bq $L^{-1}$ [1]. $^{137}Cs$ is one of the important fission products in nuclear plant, and it has a long half-life (30 years) with gamma rays. Once the high-level radioactive waste water flowed into the sea, there will be a great harm to society.

Much more attentions have focused on the removal of radionuclides in aqueous solutions. The sorption of radionuclides has been widely studied by different methods under different conditions [2–4]. The report of 2012 nano nuclear technology also recommended that chemical reaction and separation can reduce the release of fission product effectively by capturing fission products in the post-processing operation or reactor fuel assembly with nanostructured particles and mesoporous materials [5]. Ion exchange method was recognized for the treatment of $^{137}Cs$ owing to its superior performance [6, 7]. Inorganic ion exchangers have attracted much attention due to their selectivity for alkali metal ions from contaminated aqueous solutions [8]. KNiFC was an ideal inorganic ion exchange for $^{137}Cs$ [9, 10]. The preparation and the sorption behavior

of KNiFC were studied in the literature [11–14]. The sorption mechanism of KNiFC for $^{137}Cs$ has been discussed briefly [15]. In our previous experiments, we found that $Cs^+$ was just exchanged with $K^+$ in KNiFC and has the trend of moving toward face-centered clearance of KNiFC [16]. The sorption process of KNiFC for $Cs^+$ were believed to takes place through two main steps: (1) the solution phase till they reach the surface of the solid particles and (2) diffusion of the ions though the solid particles themselves [17].

Despite of the established significance of selective sorption of KNiFC for $Cs^+$, little is known about the reasons of the high selectivity. There are still some troubles for the removal of $^{137}Cs$ from highly saline solutions, especially for the coexisting cations with a similar structure to $Cs^+$. It is widely believed that the selective capacity is proportional to the size of the hydrated cations [13, 18]. However, at the initial concentrations of competitive cations 1 and 10 mmol $L^{-1}$, the $K_{d,Cs}$, value was lower when divalent cations presented than that when monovalent cations presented [14]. According to our previous studies, we think there may be other reasons such as electric charge, ionic radius, electronegativity, etc. Here, we design an experiment to examine the effect of the monovalent ($Na^+$, $K^+$, $NH_4^+$) and divalent ($Ca^{2+}$, $Mg^{2+}$) cations on $K_{d,Cs}$, from simulated high-level liquid wastes. Specifically, we have undertaken batch equilibrium experiments to generate sorption isotherms and kinetics studies in order to explore the reasons about selective sorption.

## Materials and methods

### Synthesis of KNiFC

KNiFC was prepared by the following procedures: 150 mL of 0.5 mol $L^{-1}$ $K_4[Fe(CN)_6]\cdot 3H_2O$ was added into 170 mL of 0.5 mol $L^{-1}$ $Ni(NO_3)_2\cdot 6H_2O$ slowly. After stirring for 2 h and standing for 12 h, the precipitate was washed with deionized water several times, and dried in an oven at 70 °C for 24 h. A piece mesh (9–18) was used for sorption experiments. The composition of the product was analyzed using a IRIS Intrepid direct-reading plasma spectrometer at 23 °C, and the X-ray powder diffractometry was performed using a model X'TRA from Thermo Electron Corporation.

### Sorption experiments

The high-level liquid wastes are simulated with the solution of CsCl. Kinetic and isotherm experiments of $Cs^+$ from single metal solutions were undertaken by using a batch equilibrium technique. 50 mL aqueous solution containing 0.075 mol $L^{-1}$ $Cs^+$ was mixed with 0.07 g KNiFC at 25 °C for 8 h to assure equilibrium. After equilibration, the aqueous solution was centrifuged with centrifuge at $4 \times 10^3$ rpm for 15 min. Then the concentration of the supernatant was measured using an ICE 3000 atomic absorption spectrophotometer (AAS) at 26 °C and the solid was characterized using a X'TRA X-radial Diffractometer from Thermo Electron Corporation. The distribution coefficient of $Cs^+$, $K_{d,Cs}$ (ml $g^{-1}$), was determined as:

$$K_{d,Cs} = \frac{C_0 - C}{C}\left(\frac{V}{M}\right) \quad (1)$$

where $C_0$ (mmol $L^{-1}$) is the initial concentration of $Cs^+$ in the solution, $C$ (mmol $L^{-1}$) is the concentration at equilibrium, $V$ (mL) is the volume of solution, and $M$ (g) is the mass of adsorbent.

### Sorption models and statistical analysis

In the present study, different mathematical models were applied to $Cs^+$ sorption in batch experiments to obtain comparable and physically interpretable parameters, which describe the sorption process. Vasanth Kumar has shown that non-linear method could be a better way to obtain the parameters than the linear method for sorption isotherm [19]. Here, non-linear regression analysis was chosen to obtain the model parameters with Origin Pro_7.5. Non-linear regression method was based on the Levenberg–Marquardt algorithm, which is the algorithm most widely used in non-linear least squares fitting. The coefficient of determination ($R^2$), mean squared error (RMSE) and standard error of the estimate (SEE) were used to estimate the goodness of the fit of the studied models:

$$R^2 = \frac{\sum_1^n (q_{re} - q)^2}{\sum_1^n (q_{exp} - q)^2} \quad (2)$$

$$RMSE = \sqrt{\frac{\sum_1^n (q_{exp} - q_{re})^2}{(n-2)^2}} \quad (3)$$

$$SEE = \sqrt{\frac{1}{n-p}\sum_1^n (q_{re} - q_{exp})^2} \quad (4)$$

where $q_{re}$ is the calculated (predicted) value of the dependent variable, $q_{exp}$ is the experimental (observed) value of the dependent variable, $q$ is the average of all observed values of the dependent variable, $n$ is the number of observations, and $p$ is the number of parameters in the regression model. A smaller RMSE and SSE values and a higher $R^2$ values indicate a better regression model.

## Results and discussion

### Structure characterization

Figure 1a showed the XRD pattern of the solid before sorption. All the peaks can be readily indexed to the standard pattern $K_2NiFe(CN)_6$. After sorption, the initial pattern changed and conformed to $Cs_2NiFe(CN)_6$ well, which was shown in Fig. 1b. The diffraction intensity of $K_2NiFe(CN)_6$ is higher than $Cs_2NiFe(CN)_6$ for the same indices of crystal face (*h k l*) and the first strong peak became weak. A new diffraction peak appeared at 30.6874°, while one diffraction peak disappeared at 54.9548°. $K^+$ was exchanged by $Cs^+$ in the sorption process and the radius of $Cs^+$ is larger than $K^+$, thus the size of unit cell became larger after sorption and the shorter distance with change site will have more influence on the diffraction face. From all the phenomena mentioned above, the structure of KNiFC changes after sorption.

### Sorption kinetic

Sorption kinetic was investigated by the batch method. The whole sorption processes can be predicted by fitting pseudo-fist order and pseudo-two order. The pseudo-fist order equation is given as:

$$q_t = q_e(1 - e^{-k_1 t}) \tag{5}$$

where $q_e$ (mg $g^{-1}$) is the amount of $Cs^+$ taken up in solid phases at equilibrium, $q_t$ (mg $g^{-1}$) is the amount of $Cs^+$ taken up in solid phases at any time $t$ (h), and $K_1$ is the rate constant of sorption.

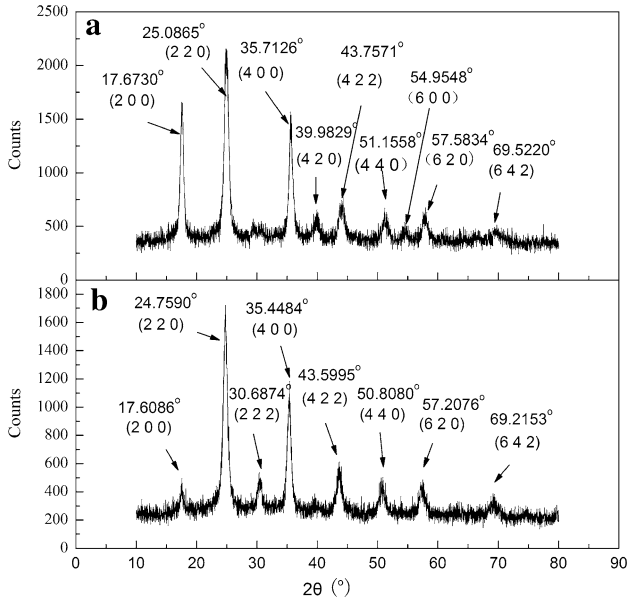


**Fig. 1** The XRD patterns of solid before (**a**) and after sorption (**b**), indices of crystal face (h k l),corresponding $2\theta$ values at peak positions

The pseudo-second order equation is given as:

$$q_t = \frac{k_2 q_e^2 t}{1 + k_2 q_e t} \tag{6}$$

where $q_e$ (mg $g^{-1}$) and $q_t$ (mg $g^{-1}$) are the amount of $Cs^+$ taken up in solid phases at equilibrium and any time $t$ (h) respectively, and $K_2$ is the rate constant of sorption.

The data was fitted with the two models respectively. The $R^2$, RMSE and SSE for each model were listed in Table 1. According the Table 1, pseudo-second order fitted the sorption process better than pseudo-first order. A non-linear relation of pseudo-second order was obtained from the plot of $q_t$ versus $t$ as seen in Fig. 2. We preliminarily concluded that the rate limiting step may be chemical sorption involving valency forces through sharing or exchange of electrons between KNiFC and CsCl.

### Adsorption mechanism

The ion exchange process was controlled by three steps [2]: (1) diffusion of $Cs^+$ through the solution film surrounding the KNiFC particles is called film diffusion, (2) diffusion of $Cs^+$ through the hydrated interlayer space of the KNiFC particle is defined intraparticle diffusion, and (3) chemical exchange reaction of $Cs^+$ at the particle surface is referred as chemical reaction [17]. Generally, the kinetic models just describe the whole sorption process, but the actual rate limiting steps in the adsorption process are not provided in detail. That can be explained by the different models such as Weber and Morris intraparticle diffusion model [20], Boyd kinetic plot [21] and shrinking core model [22, 23]. For a solid–liquid sorption process, adsorption transfer is usually characterized by either film diffusion, intraparticle diffusion or both two.

Weber and Morris intraparticle diffusion equation is given as follows:

$$q_t = K_m t^{1/2} + D \tag{7}$$

where $q_t$ (mg $g^{-1}$) is the amount of $Cs^+$ taken up in solid phases at any time $t$ (h), $K_m$ (mg $g^{-1}$ $h^{-0.5}$) is the intraparticle diffusion rate coefficient, and $D$ (mg $g^{-1}$) is the liquid film thickness. The larger the value of $D$ values, the greater the effect for the boundary layer in the sorption process. If intraparticle diffusion is the rate limiting step in the sorption process, then the plot of $q_t$ versus $t^{1/2}$ should be a straight line and pass through the origin.

As shown in Fig. 3, the plots possess two linear portions, which indicate that these two steps may influence the sorption process. The first linear portion of the plot indicated the boundary layer had an effect on the sorption of the KNiFC for $Cs^+$, and the second linear portion of the

**Table 1** Sorption reaction model parameters of $Cs^+$ on KNiFC obtained by using non-linear regression analysis their statistical characteristics

| Sorption reaction model | Parameters ± SE | $R^2$ | RMSE | SEE |
|---|---|---|---|---|
| Pseudo-first order | $q_e = 484 \pm 45$ | 0.989 | 16.79 | 2,255 |
| | $K_1 = 0.60 \pm 0.114$ | | | |
| Pseudo-second order | $q_e = 644 \pm 26$ | 0.994 | 0.00003 | 7.313 |
| | $K_2 = 0.00084 \pm 0.000024$ | | | |

*SE* error on parameter value, $R^2$ the coefficient of determination, *RMSE* the discrete degree of sample, *SEE* error of the estimate

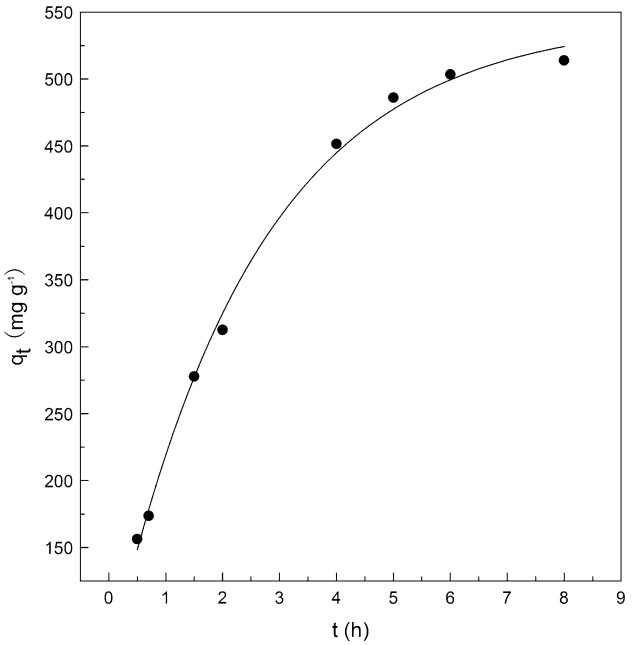


**Fig. 2** The sorption kinetic of KNiFC for $Cs^+$ as a function contact time $t$, initial CsCl concentration 0.075 mol $L^{-1}$, solid/liquid ratio 1.44 mg $L^{-1}$, initial pH 5.8, temperature 25 °C

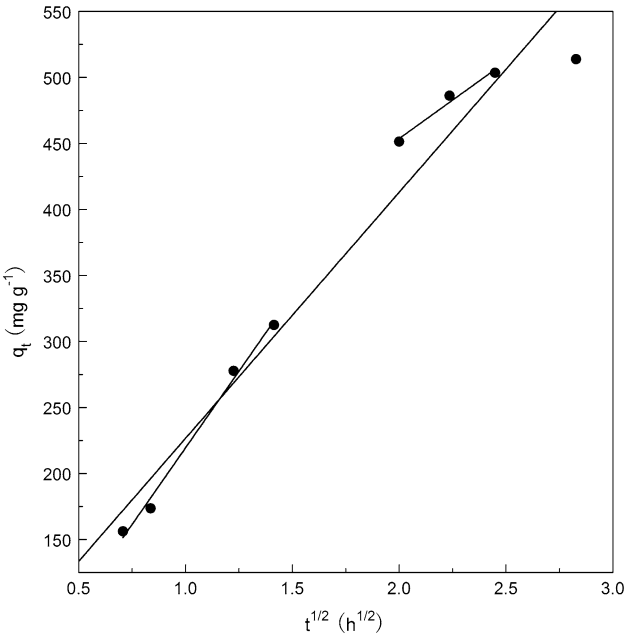


**Fig. 3** Intraparticle diffusion model plots for $Cs^+$ by KNiFC as a function contact time $t^{1/2}$, initial CsCl concentration 0.075 mol $L^{-1}$, solid/liquid ratio 1.44 mg $L^{-1}$, initial pH 5.8, temperature 25 °C

plot indicated the intraparticle diffusion taken place in the KNiFC. This deviation from the origin indicates that the liquid film diffusion may be involved in controlling the sorption of $Cs^+$ on KNiFC.

The kinetic data was analyzed with the Boyd kinetic model to predict the actual rate limiting step in the sorption process, and the results are shown in Fig. 4. The Boyd kinetic model is given as:

$$\frac{q_t}{q_e} = F = 1 - \frac{6}{\pi^2}\exp^{(-kt)} \quad (8)$$

Equation (8) can be rearranged into the following form:

$$kt = -0.4977 - \ln(1 - F) \quad (9)$$

where $q_t$ (mg $g^{-1}$) is the amount of $Cs^+$ taken up in solid phase at any time $t$ (h), $F$ is the fraction of KNiFC for $Cs^+$ at any time $t$ and $kt$ is a mathematical function of $F$. If the plots ($kt$ vs. time $t$) are linear and pass through the origin, then the actual limiting step in the adsorption process is the intraparticle diffusion. It can be seen from Fig. 4 that the plots is neither linear nor passing through the origin, which indicated that the sorption process of KNiFC for $Cs^+$ is controlled primarily by film diffusion and intraparticle diffusion together. Therefore, there may not be any rate limiting sorption processes of KNiFC for $Cs^+$. However, according to the reaction rate coefficient $k_m$ (1.4016) and $k$ (0.153115), the rate limiting processes of sorption for $Cs^+$ was controlled by film diffusion.

## Sorption isotherms

The sorption of KNiFC for $Cs^+$ was studied in the concentration range 0.015–0.1 mol $L^{-1}$. Equilibrium data, the well-known sorption isotherms, reveals the specific relation between the concentration of adsorbate and its sorption degree on adsorbent surface at constant temperature [14].

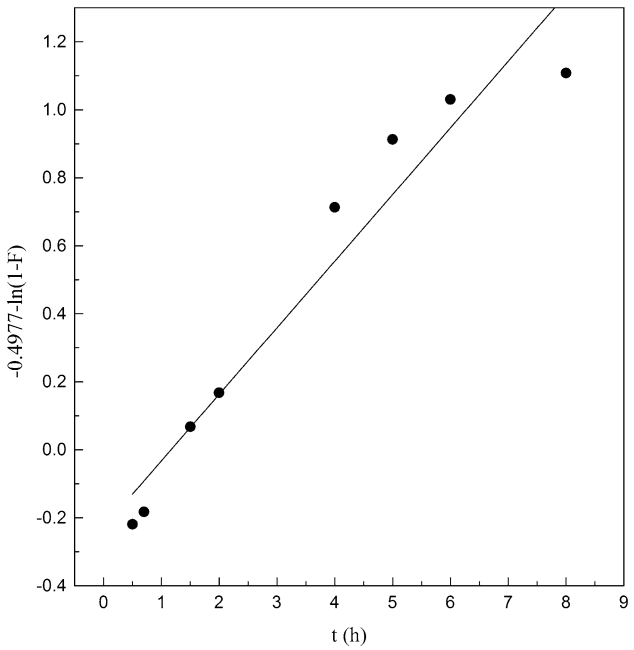


**Fig. 4** Boyd kinetic model plots for $Cs^+$ by KNiFC as a function contact time *t*, initial CsCl concentration 0.075 mol $L^{-1}$, solid/liquid ratio 1.44 mg $L^{-1}$, initial pH 5.8, temperature 25 °C

In this present study, the equilibrium experimental data about the sorption of KNiFC for $Cs^+$ was analyzed by using the Langmuir and Freundlich isotherms. The Langmuir equation is given by

$$q_e = \frac{q_{max} b C_e}{1 + b C_e} \quad (10)$$

where $C_e$ (mmo1 $L^{-1}$) and $q_e$ (mmol $g^{-1}$) are the equilibrium concentrations of $Cs^+$ in the aqueous solution and solid phase, respectively. $q_{max}$ (mmol $g^{-1}$) is the maximum amount of $Cs^+$ taken up in solid phase. *b* (L $mmol^{-1}$) is the Langmuir constant.

The Freundlich equation is given by

$$q_e = K_F C_e^{1/a} \quad (11)$$

where $C_e$ (mmo1 $L^{-1}$) and $q_e$ (mmol $g^{-1}$) are the equilibrium concentrations of $Cs^+$ in the aqueous solution and solid phase, respectively. $K_F$ (L $mmol^{-1}$) is constant related to the sorption capacity which represents the affinity between the adsorbate and adsorbent. The $1/a$ (non dimensional) is an empirical parameter related to the sorption intensity, which varies with the heterogeneity of the adsorbent.

The data was fitted to Langmuir and Freundlich model. The $R^2$, RMSE and SSE for each model was calculated and listed in Table 2. Both Langmuir and Freundlich models fit the data well, and the maximum exchange capacity is approximate to 223.4 mg $g^{-1}$. The sorption of KNiFC for $Cs^+$ was described by Freundlich isotherm better than Langmuir isotherm, which indicated a chemisorption sorption on heterogeneous surfaces.

**Table 2** Isotherm model parameters of cesium ions sorption on KNiFC obtained by using non-linear regression analysis and their statistical characteristics

| Isotherm model | Parameters ± SE | $R^2$ | RMSE | SSE |
|---|---|---|---|---|
| Langmuir | $b = 0.058 \pm 0.043.$ | 0.9344 | 0.0595 | 0.0179 |
| | $q_{max} = 1.68 \pm 0.036$ | | | |
| Freundlich | $K_F = 0.36 \pm 0.069$ | 0.9421 | 0.0577 | 0.0155 |
| | $1/a = 0.31 \pm 0.048$ | | | |

*SE* error on parameter value, $R^2$ the coefficient of determination, *RMSE* the discrete degree of sample, *SEE* error of the estimate

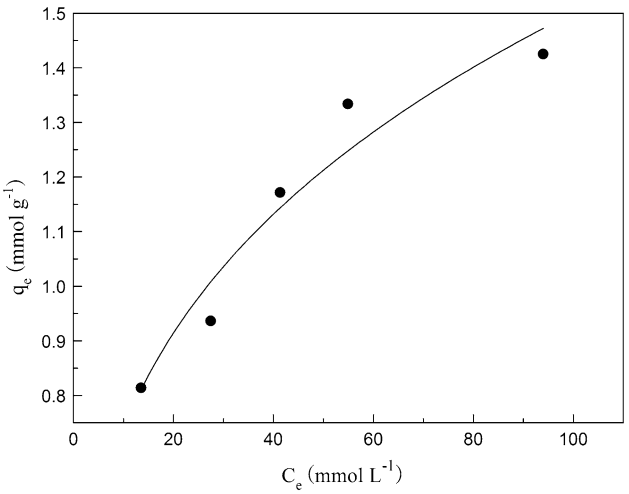


**Fig. 5** Isotherm for $Cs^+$ by KNiFC as a function $Cs^+$ equilibrium concentration $C_e$, solid/liquid ratio 1.44 mg $L^{-1}$, initial pH 5.8, temperature 25 °C

A non-linear relation was obtained from the Freundich plot as shown in Fig. 5. The value of $K_F$ was 0.36 ± 0.069, and $1/a$ was 0.31 ± 0.048 after fitting. The value of $1/a < 1$ reflected the situation at higher concentration of adsorbate, it becomes increasingly difficult to adsorb additional molecules. This may be attributed to two reasons: the specific binding sites become filled and remaining sites are limited to the ions.

## Effect of pH on $K_{d,Cs}$

The effect of pH on the sorption of $Cs^+$ from aqueous solutions was investigated over the pH range of 1.7–6.5. The results are shown in Fig. 6. The distribution coefficient of KNiCF for $Cs^+$ was found to decline with the increase of pH to a minimum value of 5.3 and then increase with the increase of pH. Similar results were reported by Jukka et al. [15], which agreed with the regulation that compared with alkali environment, the distribution coefficient increase

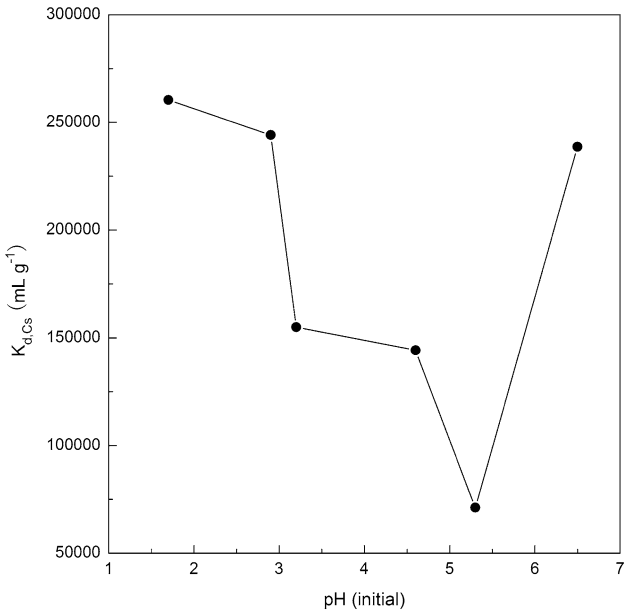


**Fig. 6** The distribution coefficient of $Cs^+$ as a function initial pH, initial $Cs^+$ concentration 0.87 mmol $L^{-1}$, solid/liquid ratio 1.44 mg $L^{-1}$. *Each point* is the arithmetic mean of three data

**Table 3** The relevant parameters of $Cs^+$, $NH_4^+$, $K^+$, $Na^+$, $Mg^{2+}$, $Ca^{2+}$ [24–26]

| | Hydrated radius (nm) | Ionic radius (nm) | Charge-radius ratio | Electronegativity |
|---|---|---|---|---|
| $NH_4^+$ | 0.331 | 0.148 | – | – |
| $Na^+$ | 0.358 | 0.117 | 1.05 | 1.05 |
| $K^+$ | 0.331 | 0.149 | 0.75 | 0.75 |
| $Cs^+$ | 0.329 | 0.186 | 0.59 | – |
| $Ca^{2+}$ | 0.412 | 0.100 | 2.02 | 2.02 |
| $Mg^{2+}$ | 0.428 | 0.072 | 3.08 | 1.2 |

with the increase of pH in acidic environment because of the competition of $H^+$ with $Cs^+$ for the exchange sites in the adsorbent. The reason needs to be investigated systematically in our further work.

Effect of cations on $K_{d,Cs}$

The effect of coexistence cations on $K_{d,cs}$ was studied. The common cations in radioactive wastewater, including monovalent ($NH_4^+$, $K^+$, $Na^+$) cations and divalent ($Ca^{2+}$, $Mg^{2+}$) cations, were chosen. Futhermore, $NH_4^+$, $K^+$ and $Na^+$ are similar as $Cs^+$ on physical properties. The values of $K_{d,cs}$ for $Cs^+$ in absence and presence of $NH_4^+$, $K^+$, $Na^+$, $Mg^{2+}$ and $Ca^{2+}$ are 38,026, 1,825, 2,531, 16,281, 31,635 and 11,966 mL $g^{-1}$, respectively, while keeping constant the $Cs^+$ initial concentration 0.1 mol $L^{-1}$. It can be found that the interference rejection capability for $Cs^+$ sorption followed the order of $NH_4^+ > K^+ > Na^+ > Ca^{2+} > Mg^{2+}$. The value of hydrated ionic radius, ionic radius, charge-radius ratio, and electronegativity of $NH_4^+$, $K^+$, $Na^+$, $Mg^{2+}$ and $Ca^{2+}$ was listed in Table 3. After comparing, the result agrees with the order of the size of hydrated cations basically. The film diffusion relates to the hydrated ionic radius and charge-radius ratio. At the same time, the metals get through the KNiFC in the form of ion. Herein, the rate limiting processes was controlled mainly by film diffusion. Therefore the selective sorption of KNiFC for metal ions is not only depended on the hydrated radius, but ionization potential and the structure of KNiFC.

## Conclusion

The sorption behavior was fitted well by Freundlich isotherm and pseudo-second-order. The sorption process was controlled collectively by film diffusion and intrapartical diffusion. But, the rate limiting steps was controlled by film diffusion, which pointed the way to improve the whole exchange rate by improving film diffusion rate. The interference rejection capability for $Cs^+$ sorption was found to follow the order of $NH_4^+ > K^+ > Na^+ > Ca^{2+} > Mg^{2+}$. The hydrated radius, charge-radius ratio, ionization potential and the structure of KNiFC have an effect on the diffusion rate, which may lead to the selective diffusion. The environmental factors, such as pH and temperature, have a significant influence on the physico-chemical property of adsorbent and adsorbate. Therefore, we may improve the selective separation of KNiFC for $Cs^+$ with coexisting cations by setting different parameter values for the solution. The distribution coefficient $K_{d,Cs}$ was found to decline with the increase of pH to a minimum value of 5.3 and then increase with the increase of pH, which may provide an evidence for avoiding the range of pH in the sorption process of KNiFC for $Cs^+$.

**Acknowledgments** This work was financially supported by the National Natural Foundation of China (11105073, 81101146), the Natural Science Foundation of Jiangsu Province (BK2011739, BK2011738, No. BK2012799) and the Ph.D. Programs Foundation of Ministry of Education of China (No. 2012321811008).

## References

1. Fukushima Daiichi NPS Prompt Report (2013) Tokyo Electric Power Company, Tokyo. http://www.tepco.co.jp/en/press/corp-com/release/2013/1229861_5130.html. Accessed 19 Aug 2013
2. Montana M, Camacho A, Serrano I, Devesa R, Matia L, Valles I (2013) Removal of radionuclides in drinking water by membrane treatment using ultrafiltration, reverse osmosis and electrodialysis reversal. J Environ Radioact 125:86–92

3. Park YJ, Lee YC, Shin WS, Choi SJ (2010) Removal of cobalt, strontium and cesium from radioactive laundry wastewater by ammonium molybdophosphate–polyacrylonitrile (AMP–PAN). Chem Eng J 162:685–695
4. Yu SM, Zha CC, Lu FF (2013) Simultaneous separation of simulated radionuclides strontium and neodymium using in situ hydrotalcite synthesis. J Radioanal Nucl Chem 298:877–882
5. The 2012 nanonuclear workshop (2012) TMS, Maryland. http://www.tms.org/meetings/2012/nanonuclear/background.aspx. Accessed 7 June 2012
6. Hattori H, Alabi WO, Jermy BR, Aitani AM, Al-Khattaf SS (2013) Pathway to ethylbenzene formation in side-chain alkylation of toluene with methanol over cesium ion-exchanged zeolite X. Catal Lett 143:1025–1029
7. Parab H, Sudersana M (2010) Engineering a lignocellulosic biosorbent-coir pith for removal of cesium from aqueous solutions: equilibrium and kinetic studies. Water Res 44:854–860
8. Jiang J (2012) Study of an inorganic ion exchanger $Mg_2Ti_{1.25}(PO_4)_3$. Adv Mater 442:50–53
9. Kazemian H, Zakeri H, Rabbani MS (2006) Cs and Sr removal from solution using potassium nickel hexacyanoferrate impregnated zeolites. J Radioanal Nucl Chem 268:231–236
10. Mimura H, Kimura M, Akiba K, Onodera Y (1999) Selective removal of cesium from sodium nitrate solutions by potassium nickel hexacyanoferrate-loaded chabazites. Sep Sci Technol 34:17–28
11. Mimura H, Kageyama N, Akiba K (1998) Ion-exchange properties of potassium nickel hexacyanoferrate(II) compounds. Solvent Extr Ion Exch 16:1013–1031
12. Kubica B, Godunowa H, Tuteja-Krysa M, Stobinski M, Misiak R (2004) Sorption of lead(II) on transition metal hexacyanoferrates(II) and on nickel(II)-potassium hexacyanoferrate(II) resin composite in hydrochloric acid medium. J Radioanal Nucl Chem 262:721–724
13. Du ZH, Jia MC, Wang WX (2013) Cesium removal from solution using PAN-based potassium nickel hexacyanoferrate(II) composite spheres. J Radioanal Nucl Chem 298:167–177
14. Vrtoch L, Pipiska M, Hornik M, Augustin J, Lesny J (2011) Sorption of cesium from water solutions on potassium nickel hexacyanoferrate-modified Agaricus bisporus mushroom biomass. J Radioanal Nucl Chem 287:853–862
15. Jukka L, Rsto H (1997) Ion exchange of cesium on potassium nickel hexacyanoferrate(II)s. J Nucl Sci Technol 34:484–489
16. Qing YH, Kang B, Dai YD, LI J, Sheng WT (2014) Sorption mechanism analysis of cesium ions in nickel hexacyanoferrate. Energy Sci Technol 48:1901–1906
17. Ismail IM, El-Sourougy MR, Abdel Moneim N, Aly HF (1999) Equilibrium and kinetic studies of the sorption of cesium by potassium nickel hexacyanoferrate complex. J Radioanal Nucl Chem 240:59–67
18. Awuala MR, Suzukia S, Taguchib T, Shiwakua H, Okamotoa Y, Yaitaa T (2014) Radioactive cesium removal from nuclear wastewater by novel inorganic and conjugate adsorbents. Chem Eng J 242:127–135
19. Vasanth Kumar K, Sivanesan S (2005) Prediction of optimum sorption isotherm: comparison of linear and non-linear method. J Hazard Mater 126:198–201
20. Hasany SM, Khurshid SJ (1999) Sorption behavior of Sn(II) onto Haro river sand from aqueous acidic solutions. J Radioanal Nucl Chem 240:25–29
21. Kumar PS, Ramalingam S, Abhinava RV, Kirupha SD, Murugesan A, Sivanesan S (2012) Adsorption of metal ions onto the chemically modified agricultural waste. Clean Soil Air Water 40:188–197
22. Sato T, Tamura K, Okuwaki A (1992) Corrosion behaviour of silicon carbide ceramics in caustic alkaline solutions at high temperature. Br Ceram Trans 91:181–185
23. Lewandowski Z, Roe F (1994) Diffusivity of $Cu^{2+}$ in calcium alginate gel beads: recalculation. Biotechnol Bioeng 43:186–187
24. Vesselin D, Takayuki K (2012) Correlation among electronegativity, cation polarizability, optical basicity and single bond strength of simple oxides. J Solid State Chem 196:574–578
25. Volkov AG, Paula S, Deamer DW (1997) Two mechanisms of permeation of small neutral molecules and hydrated ions across phospholipid bilayers. Bioelectrochem Bioenerg 42:153–160
26. Chen NY, Lu WC, Yang J, Li GZ (2004) Support vector machine in chemistry. World Scientific Pub Co Inc, Singapore